Journal of Applied Polymer Science

Utilization of ramon seeds (*Brosimum alicastrum swarts*) as a new source material for thermoplastic starch production

Carlos Rolando Ríos-Soberanis,[1] Raciel Javier Estrada-León,[2] Víctor Manuel Moo-Huchin,[2] María José Cabrera-Sierra,[1] José Manuel Cervantes-Uc,[1] Luis Arturo Bello-Pérez,[3] Emilio Pérez-Pacheco[2]

[1]Centro De Investigación Científica De Yucatán, A.C. Unidad de Materiales, Calle 43, No. 130 x 32 y 34, Colonia Chuburná de Hidalgo C.P. 97205, Mérida Yucatán, México

[2]Instituto Tecnológico Superior De Calkiní En El Estado De Campeche, Cuerpo Académico Bioprocesos, Av. Ah Canul S/N por Carretera Federal C.P. 24900, Calkiní Campeche, México

[3]Instituto Politécnico Nacional, Centro de Desarrollo de Productos Bióticos, Kilometro 8.5 Carretera Yautepec-Jojutla, Colonia San Isidro CP 62731, Yautepec Morelos, México

Correspondence to: E. Pérez-Pacheco (E-mail: eperez@itescam.edu.mx)

ABSTRACT: The development and characterization of biodegradable polymers deriving from renewable natural sources has attracted much attention. The aim of this work was to partially characterize a thermoplastic starch obtained from the starch of seeds from the ramon tree (TPS-RS) as an option to substitute thermoplastic starch from corn (TPS-CS), in some of its applications. At 55% of relative humidity (RH), TPS-RS had higher tensile strength and deformation than TPS-CS. X-ray diffraction analysis showed similar values in residual crystallinity (percentage of crystallinity that remains after plasticization process) in both TPS. The SEM micrographs showed a few remnant granular structures in the TPS-RS. The FTIR showed a greater intensity in band at 1016 cm^{-1} in the TPS-CS and TPS-RS in comparison with their corresponding native starch, indicating an increase in the amorphous region after plasticization. The TGA analysis showed greater thermal stability in TPS-CS (340 °C) compared with TPS-RS (327 °C). In addition, the glass transition temperature in both TPS was 24 °C. The results obtained represent a starting point to potentialize the use of TPS-RS instead of TPS-CS for the development of new biodegradable materials for practical applications in different areas. © 2016 Wiley Periodicals, Inc. J. Appl. Polym. Sci. **2016**, *133*, 44235.

KEYWORDS: biodegradable; biopolymers and renewable polymers; polysaccharides

Received 18 December 2015; accepted 23 July 2016

DOI: 10.1002/app.44235

INTRODUCTION

In recent decades, growing environmental consciousness has encouraged the development of biodegradable materials from renewable resources.[1] Materials based on polysaccharides are mostly ecological because they can degrade without leaving behind ecologically harmful residues, in contrast to those which are made from synthetic polymers.[2] Among plant-derived materials, starch offers several advantages as a raw material for packaging, agricultural, and biomedical applications, including its low cost, availability as a renewable resource, non-toxicity, and biodegradability.[3]

Currently, the main sources of starch for the manufacture of biodegradable materials are corn, potato, yucca and banana, among others,[4] starch corn being the commonly used polymer in the manufacture of thermoplastic starch (TPS) for industries such as BIOP Biopolymer, Cardia bioplastics, Cerestech and Novamont, among others.[5] However, in many parts of the world, this product of agricultural origin are the main food source for the inhabitants; therefore, researchers are particularly interested in the search for starch from unconventional sources, which are not used as food for the population, and in this way exploit unused natural resources in diverse areas.[6–9] In this sense, the seeds of the ramon tree, a very abundant natural resource in the southeast of Mexico, are a unconventional source of native starch which is not used for human consumption. This polysaccharide is characterized by its high purity grade (92.5%) with an amylose content of 25.3% and a gelatinization temperature of 83 °C. The native starch granule of the ramon is oval-spherical with a size varying between 6.5 and 15

Additional Supporting Information may be found in the online version of this article.

μm. Compared with native corn starch, the native starch of ramon presents a darker color, greater water absorption, higher swelling power and high syneresis.[10] Ramon starch was proposed as a thickening and gelling agent in food, an excipient in pharmaceutical solid forms, and as biodegradable polymers for food packaging.[11]

Formation of TPS requires disruption of starch granules and their supramolecular structures by processing under high temperature and shear conditions in presence of plasticizers.[12,13] TPS can easily be adapted to different processes employing standard equipment used for synthetic polymers such as extrusion, blowing, injection, and compression molding. TPS is compatible with the environment; it is a renewable material and can be incorporated into soil as an organic fertilizer.[14,15]

The development and characterization of biodegradable polymers deriving from renewable natural sources has been receiving much attention of late and thus the starch from the seeds of the ramon tree is proposed as material for the production of these polymers.

To the best of our knowledge there are no reports about TPS obtained from ramon starch; thus the properties of the developed materials should be studied. This one is an interesting application for this non-conventional starch since it could impulse its crop and will provide greater added value. The aim of the present work was to determine the physicochemical and mechanical properties of thermoplastic starch from the ramon tree (TPS-RS) as a starting point to substitute thermoplastic starch from corn (TPS-CS) in some of its applications. Therefore, in this study, the properties of TPS-RS and TPS-CS were compared.

EXPERIMENTAL

Materials

Ramon starch was extracted as reported by Pérez-Pacheco *et al.*[10] Briefly, the starch obtained by allowing the flour to settle in a suspension of sodium bisulfite ($NaHSO_3$) and sodium hydroxide (NaOH) was subsequently sifted and centrifuged to obtain the polysaccharide. Corn starch was also used as reference and was supplied by Drogueria Cosmopolita (Mexico City). Sodium bisulfite and sodium hydroxide were purchased from Sigma-Aldrich. Corn starch is the most commonly used raw material in the elaboration of biodegradable packaging (milk chocolates and organic tomatoes) and is also the most studied material in the area of preparation and characterization of thermoplastic starch.[16–18]

Plasticization of the starch was carried out using glycerol with a purity of 98%. The water content of the starches used to produce the TPS was 10%.

Preparation of Thermoplastic Starch

Following the process described by Huang *et al.*[19] and Ma *et al.*,[20] the ramon starch was pre-mixed with glycerol (70:30, p/p) in a Black and Decker (Towson, Maryland, USA) high speed mixer blender (around five minutes) to reduce the formation of lumps in the system. The corn starch was also pre-mixed following the same process. In both cases, the resulting mixture was stored in sealed polypropylene containers for 72 h at a temperature of 20 °C, after which the pre-mixture was processed in a one-zone mixing chamber provided with a PLASTICORDER, model PLE-330, at 50 rpm and a temperature of 130 °C.

TPS films were obtained by thermo-compression using a hydraulic press. For the formation of thermoplastic starch films, a stainless steel mold (120 mm × 120 mm × 1 mm) was used in a Carver semiautomatic press with heating plates and a water circulation cooling system. Molding was performed at a temperature of 160 °C and a pressure of 48.3 MPa for 8 min; finally, the mold was removed and the specimen dimensions (Type IV) for tensile tests adjusted to ASTM D638 standard.

Moisture Absorption of Films

The tensile test samples were conditioned to several relative humidity (RH) controlled environments (33 and 55%) at a constant temperature of 25 °C until ready for testing. Desiccators were used as conditioning chambers. The different relative humidity environment chambers were obtained using several saturated salts and were selected according to the recommendations given in ASTM E104-51 and ASTM E104-85 standards. Potassium acetate and magnesium nitrate hexahydrate were used for the 33% RH and 55% RH, respectively. A digital hygrometer was placed inside each chamber to measure and continuously monitor the temperature and relative humidity.

The weight gain of the test specimens after exposure to the selected relative humidity environments was measured as a function of time. The moisture absorption was estimated using the eq. (1).

$$M = \frac{M_w - M_d}{M_d} \times 100 \quad (1)$$

where M is the percentage of absorbed moisture, M_w is the weight of the wet sample, and M_d is the weight of the dry sample.

Mechanical Testing

The mechanical properties for tensile loadings were determined using specimens according to the ASTM standard D-638. The specimens were tested in a uniaxial tension test using a Universal Testing Machine, Shimadzu model AG-I equipped with a load cell of 1000 N. The samples were tested using a crosshead speed of 5 mm/min.

Dynamic Mechanical Analysis

Dynamic mechanical analysis (DMA) as a function of temperature was conducted using a DMA-7 from Perkin Elmer in the extension mode. Rectangular specimens of 15 mm × 4 mm × 1.2 mm from TPS-RS and TPS-CS were subjected to a static force of 400 mN and a dynamic force of 320 mN at 1 Hz. The tan δ was determined in the temperature range between −100 °C and 80 °C at a heating rate of 3 °C/min.

Scanning Electron Microscopy

The fracture surfaces of the TPS specimens subjected to tensile testing were analyzed morphologically by means of a scanning electron microscope (SEM), model JEOL JSM-6360LV operated at 10 kV. The samples were coated with a layer of pulverized gold prior to analysis.

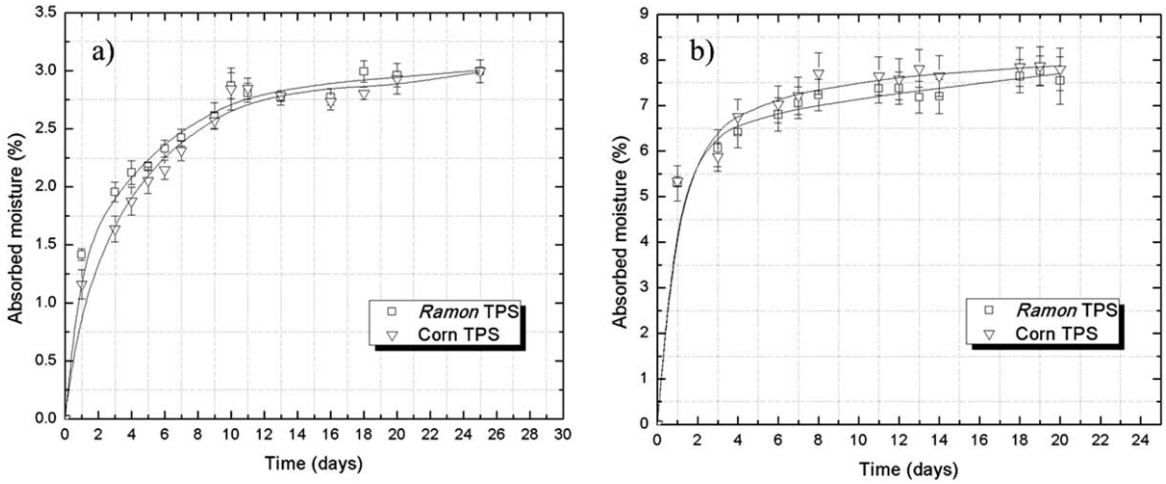

Figure 1. Isotherms of moisture absorption for *Ramon* and corn TPS (a) 33% of relative humidity, (b) 55% of relative humidity.

Attenuated Total Reflectance Fourier Transform Infrared Spectroscopy

Fourier transform infrared (FTIR) spectrometry equipment Nicolet 8700 was used equipped with a ZnSe attenuated total reflectance (ATR) accessory. Scans in the 4000 and 650 cm^{-1} spectral range were performed and the spectra registered after averaging 100 scans with a resolution of 4 cm^{-1}.

X-ray Diffraction

After 10 days of conditioning in an environment of 55% RH and a moisture content of 7%, films were submitted to X-ray radiation using a Siemens diffractometer, model D-5000, operating at Cu Kα radiation wavelength (λ = 1.79018 Å), 40 kV, 30 mA, and sampling interval of 0.02°. Scattered radiation was detected in the angular range of 5–35 °C (2θ).

Relative crystallinity for the TPS samples was calculated with eq. (2), following the method established by Nara and Komiya.[21]

$$C_{\%} = \left(\frac{A_C}{A_C + A_A}\right) \times 100 \quad (2)$$

where $C_{\%}$ denotes the percentage of crystallinity, A_C the area of the crystalline region, and A_A the area of the amorphous region.

The areas of the diffractograms were calculated using Autocad software version 2015.

Thermogravimetric Analysis

Thermogravimetric analysis (TGA) was carried out using a TGA Perkin–Elmer 7 instrument under nitrogen flow of 50 mL min^{-1} and at a heating rate of 10 °C min^{-1}. The temperature scans were performed from 50 °C to 500 °C.

RESULTS AND DISCUSSION

Moisture Content

The absorption properties of any material are very important for the design and optimization of many processes such as drying, packaging and storage. TPS is hydrophilic and attracts water molecules from the surroundings when the environmental RH increases, or loses water as the RH decreases. A change in the moisture content leads to a change in the TPS structure, which will subsequently affect the mechanical and thermal properties.[22] In Figure 1 we can observe that the water absorption isotherms with respect to the storage time for TPS-RS and TPS-CS were found to be similar at 33 and 55% of RH.

The moisture absorption isotherms of TPS-RS and TPS-CS exposed to 33% RH are presented in Figure 1(a). As can be seen, during the first four days of exposure to the relative humidity, the TPS-RS and TPS-CS showed a very rapid weight increase, after which the absorption slowed down until an equilibrium moisture content of 2.7% was reached at 10 days of exposure. Figure 1(b) shows the moisture absorption isotherms of TPS-RS and TPS-CS exposed to 55% RH and once again a rapid increase in weight can be observed during the first three days of exposure to relative humidity, followed by slower absorption until an equilibrium moisture content of 7% was reached at 10 days of exposure.

The absorption curves of TPS-RS and TPS-CS were typical of water-sensitive polymers, and this can be explained by the addition of glycerol which provides more active sites by exposing its hydrophilic hydroxyl groups in which the water molecules could be absorbed. [23]

It is also well known that the moisture content depends strongly on the nature of the starch employed, relative humidity, and the conditioning period, as well as the drying conditions prior to the stabilization of the material, which is why the absorption percentages reported in the scientific literature tend to vary significantly. In this work, the estimated absorption values were similar to those reported by Curvelo *et al.*,[24] and Chen *et al.*[25] who indicated that moisture absorption in thermoplastic starch is produced primarily in the dissolution of water in the polymer network; subsequently, the water occupies the free volume in the glassy structure and finally, hydrogen bonds are generated between the hydrophilic groups of the polymer and the water.

On the other hand, it has been reported that a high content of plasticizer in thermoplastic starches generates an increase in the rate of moisture absorption, attributed to the hygroscopicity of glycerol, which allows the water molecules to be transported throughout the polymeric matrix.[24]

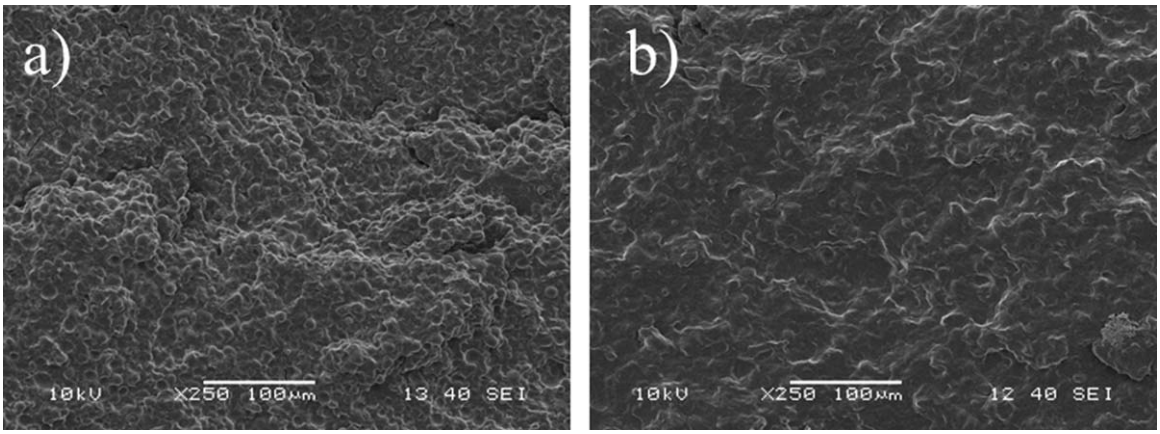

Figure 2. Scanning electron microscopy (SEM) images for the fracture surfaces of (a) *Ramon* TPS, (b) corn TPS.

Scanning Electron Microscopy

Figure 2 shows the fracture surfaces of tensile test specimens of TPS-RS and TPS-CS. The TPS-CS [Figure 2(b)] exhibited a homogenous surface, indicating that the starch granules were completely destructured. In contrast, more evident granular structures are clearly visible in the TPS-RS [Figure 2(a)] indicating that the starch granules were not completely destructured, i.e. the sample exhibits a partial thermoplasticization. Similar granular structures have been observed in yucca TPS which was denominated "ghost" granular structures.[26] This condition was most likely caused by the variation in pressure and temperature of the plates in the hydraulic press when the TPS films are being manufactured.[27] Although it should be also mentioned that the thermoplasticizing process depends on amylose and amilopectin content, type, and content of plasticizing agent, among others.[28] Similarly, it has been established that the starch granular structures remain on the fracture surface of TPS because of the use of an insufficient amount of plasticizer, since this compound controls the rupture of the granular structure.[29]

Fourier Transform Infrared Spectroscopy

FTIR spectroscopy was used to investigate the differences between the spectra of native starch and thermoplastic starch, which could indicate changes in the chemical structure associated with the mixing.

Figure 3 shows the infrared absorption spectra of TPS-RS and TPS-CS. FTIR spectra of native starch of ramon and corn were reported previously by our research group.[11] After the plasticization process with glycerol the band corresponding to the stretching of —OH groups of the native starches is slightly shifted from 3291 to 3275 cm^{-1} for TPS-RS. This is because of the formation of hydrogen bonds between the hydroxyl groups of the glycerol (plasticizing agent) and the starch. The formation of hydrogen bonds alters the force constant of the groups involved, and thus, the frequency of deformation is altered.[30] As one would expect, the FTIR spectrum of thermoplastic starch shows more intense bands in the region of 2980–2850 cm^{-1}, in comparison with those exhibited by native starch, which are associated with C-H stretching of the glycerol structure. The FTIR spectrum of the TPS-RS also presents two bands, which

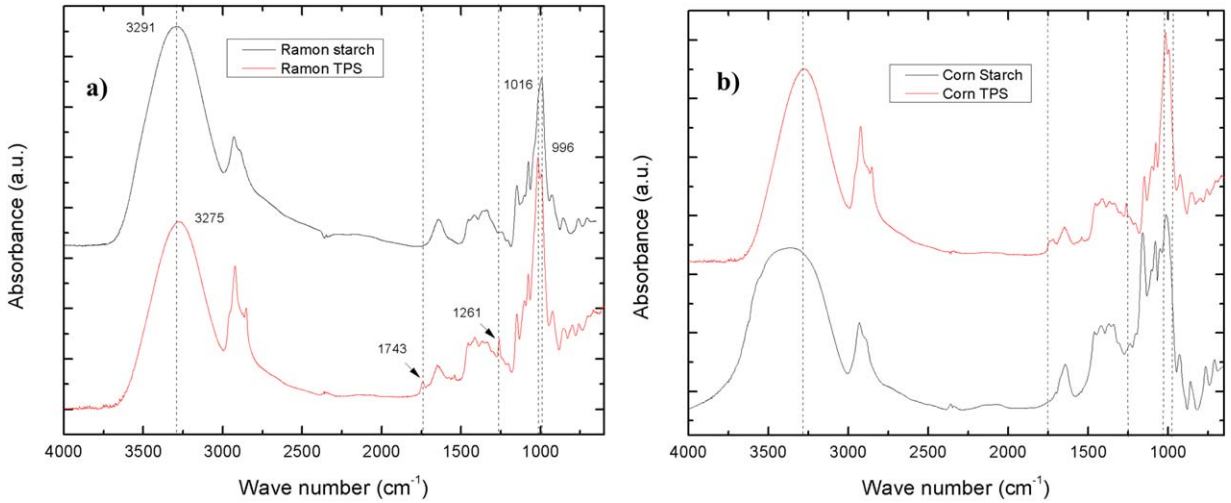

Figure 3. FT-IR spectra of (a) *Ramon* TPS and *Ramon* native starch, (b) corn TPS and corn native starch. [Color figure can be viewed in the online issue, which is available at wileyonlinelibrary.com.]

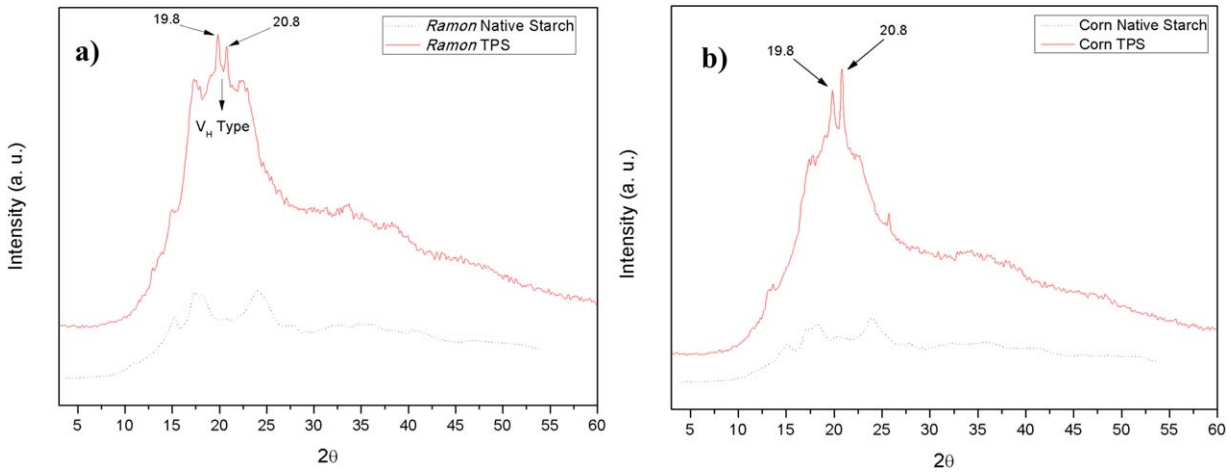

Figure 4. X-ray diffraction patterns of (a) *Ramon* TPS and *Ramon* native starch, (b) corn TPS and corn native starch. [Color figure can be viewed in the online issue, which is available at wileyonlinelibrary.com.]

cannot be observed in the native starch: 1743 and 1261 cm^{-1}. The presence of these bands has been reported previously, when the spectra of native starch and thermoplastic starch of cassava were compared.[31] The first sign was attributed to compounds with carbonyl groups originating from a slight decomposition of the glycerol, and the second to the CH_2-OH link of glycerol.

The list of intensities of the bands located at 1016 and 996 cm^{-1} present an interesting phenomenon; in the native starch, the band at 996 cm^{-1} is more intense than that observed at 1016 cm^{-1}, while in the thermoplastic starch, the opposite phenomenon can be observed. The 996 cm^{-1} peak shows low sensitivity to crystallinity, while the peak at 1016 cm^{-1} becomes more intense, depending on how amorphous the material is.[29]

X-ray Diffraction

The crystalline structure of native starches of ramon has been reported by our research group in a previous work[11]; ramon starch exhibited a C- type crystal, while corn starch showed an A- type crystal. It is well known that the crystalline structure of native starches changes radically when said starches become part of a thermoplastic starch. Double helical crystalline structures of native starches (type A, B, or C) were transformed into simple helical crystalline structures (V_H, V_A, and E_H), which are characteristics of plastified, destructured starches.[29,32,33]

Figure 4 shows the diffraction patterns for the starches, both native and thermoplastic, from the ramon [Figure 4(a)] and from corn [Figure 4(b)]. As can be seen, the characteristic peaks of the native starches (15°, 17°, 18°, 20°, 23°, and 26° for ramon and 15°, 17°, 18°, and 23° for corn) are not present in the diffractograms of the TPS, which confirms the destructuration of native starch granules (although, in the case of the ramon, a few remnant granular structures were observed by SEM [Figure 2(a)]. In addition to the above, the diffractograms of thermoplastic starches from ramon and corn present new peaks located at 17.3°, 19.8°, 20.8°, and 22.5° for the TPS-RS and at 19.8°, 20.8°, and 25.7° for the TPS-CS. As was mentioned previously, these signs are because of the formation of simple helical structures of polymeric chains, mainly amylose, generated during the plasticization process. The majority of these 2θ values (17.3°, 19.8°, 22.5°, and 25.7°) are associated with the presence of type V_H crystalline structures in the TPS; however, it is important to note that these coexist with other types of crystalline structures, such as type V_A, since both graphs present a sign at 20.8°, which is characteristic of this type of crystals.

In addition, it was possible to observe that, after the plasticization process, the area of the amorphous region of the TPS-RS diffractogram increased with respect to that reported for native starches from ramon and corn,[11] reducing the relative crystallinity [Figure 4(a)]. The ramon native starch presented an initial value of (30.56 ± 0.98)% reported previously by our group and, after the plasticization process crystallinity was seen to reduce to a value of 3.92%. A similar tendency was observed in corn starch. In this case, the native starch presented a value of (26.6 ± 0.78%)[11] and after the plasticization process a crystallinity value of 4.29% was obtained [Figure 4(b)].

The results of crystallinity percentages show that there is no significant difference between the two TPS as the value of crystallinity diminishes by approximately 80% after plasticization of native starches. It is important to note that the corn starch recrystallizes very quickly after registering a slightly higher value in crystallinity than that of the ramon.

Thermogravimetric Analysis

Figure 5 shows the results obtained from TGA analyses carried out on the TPS-RS and TPS-CS. Both samples exhibited two regions of mass loss, although in the case of the thermoplastic starch of corn, the second transition appears to be formed by the overlapping of two different events. There are a number of reports in the literature indicating that TPS samples present two[34–36] or three[37,38] transitions during their thermal degradation; the latter depending on the type of starch used and the quantity and type of plasticizer, etc. It is also possible to observe that the greatest mass loss in TPS-CS occurs at a temperature slightly higher than that registered for TPS-RS (340 vs. 327 °C); however, this tendency was also observed in native starches.

The first mass loss, located between 100 and 200 °C, has been associated mainly with the elimination of the water present in

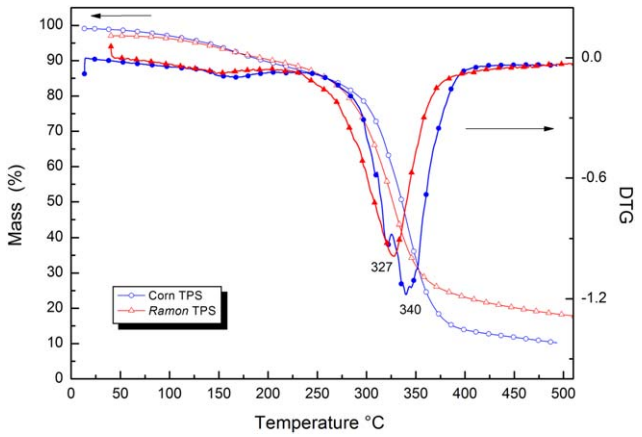

Figure 5. TGA results of the thermal decomposition and its derivative (DTG) for *Ramon* and corn TPS. [Color figure can be viewed in the online issue, which is available at wileyonlinelibrary.com.]

the TPS, although the emission of small quantities of glycerol is also possible. The second region, between 250 and 400 °C, corresponds to the thermal decomposition of the starch-glycerol system. Interestingly, no significant displacement in temperature values was observed, in which the minimums of the first derivative are obtained, in comparison with those obtained for the native starch samples. Despite this however, it is possible to appreciate that the width of the transitions in the TPS thermograms is greater than those of the native starches. This behavior could be attributed to one or more of the following factors: (i) the boiling point of glycerol (plasticizing agent) is 290 °C approximately, (ii) the addition of glycerol diminishes the interaction of both the intra- and intermolecular links of the starch-starch chains, and (iii) the strong hydrogen bond formed between the hydroxyl groups of starch chains and the glycerol molecules.[37] It is important to mention that small peaks were observed in corn TPS. This pattern could be related to small imperfection in the sample due to that some inhomogeneous or discontinuous regions are present, but for this kind of analysis they are not playing an important role. Mixing of the ingredients to produce the corn TPS should be improving.

Dynamic Mechanical Analysis

The evolution of tan δ versus temperature for TPS-RS and TPS-CS are shown in Figure 6 (graphics of storage modulus as functions of the temperature were included as supplementary material). As noted, two transitions were observed in both types of systems (corn and ramon); the first relaxation peak was located at −46 °C and the second one was centered at 24 °C. This fact is indicative of the existence of two phases which originate from the partial miscibility of glycerol and starch. The upper transition, which is the main relaxation and therefore is called α-transition, was attributed to the glass transition temperature of starch-rich phase while the lower transition, termed β-transition, was related to the glass transition of starch-poor phase, i.e. the glycerol-rich phase.[16,18,39–41] Lower transition was first detected, in DMA measurements, by Lourdin *et al.*[39] who found that this value was dependent on the concentration of plasticizer.

Mechanical Testing

The mechanical properties of TPS-RS and TPS-CS obtained at 0%, 33% and 55% of relative humidity are shown in Figure 7. It is important to note that the mechanical properties of the TPS were determined until a value of equilibrium moisture content was reached. Figure 7(a) presents the tensile strengths of TPS-RS and TPS-CS. At 0% RH, the TPS-CS and TPS-RS obtained average values of tensile strength of 4.8 MPa and 4.7 MPa, respectively; indicating that both TPS have similar values of resistance. A decrease in tensile strength of 13.5% and 18.3% was observed in TPS-CS and TPS-RS, respectively, when both materials were exposed to 33% RH. This same trend was observed in TPS exposed to 55% RH, where TPS-CS showed a drastic reduction in the tensile strength of 70.4% and in the case of TPS-RS, a reduction of 61.1%. These results indicate that the values of tensile strength of the TPS diminished as the RH increased. This has already been reported in a number of studies carried out on TPS from diverse sources.[42]

Figure 7(b) presents the elastic modulus values of TPS-RS and TPS-CS. At 0% RH, TPS-CS showed an average modulus value of 61.9 MPa while TPS-RS presented 96.4 MPa. No significant difference in the elastic modulus value was observed when the material was exposed to 33% RH. However, TPS-RS exposed to 55% RH registered an elastic modulus value of 15 MPa, which represents an 83.4% decrease of the initial value. TPS-CS presented a similar behavior; the TPS exposed to 55% RH registered a modulus value of 4 MPa, representing a loss of 92% of the initial value.

Chaleat *et al.*[42] have reported that the mechanical properties of biofilms elaborated with starch depend on the amylose-amylopectin ratio, quantity of plasticizer, quantity of water, and storage conditions. In addition to the above, these authors have also pointed out that the TPS elaborated from starches with similar amylose contents can present differences in their tensile strength. The latter is mainly attributed to small variations in the quantity of crystalline type-B structure; the presence of this type of crystallinity is known to increase rigidity and resistance to rupture in TPS. Moreover, these properties are also affected

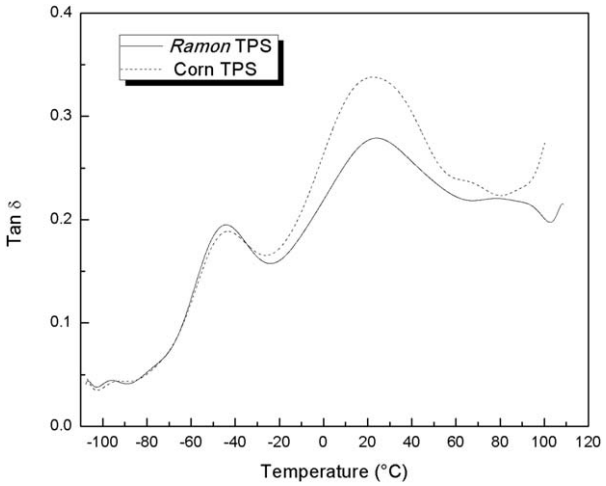

Figure 6. DMA Plots of tan δ versus temperature for *Ramon* and corn TPS.

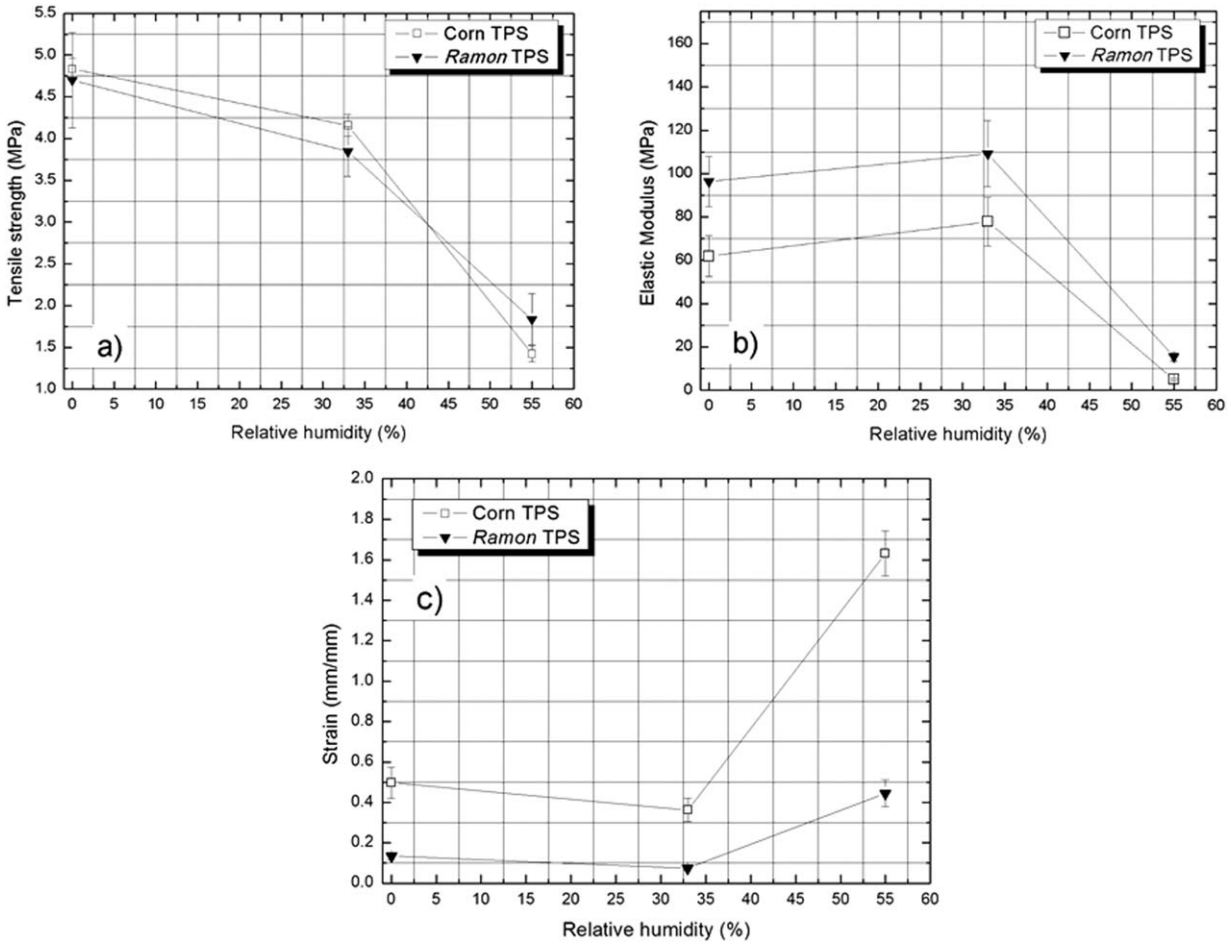

Figure 7. Mechanical properties versus relative humidity for *Ramon* and corn TPS. (a) tensile strength, (b) elastic modulus, (c) strain.

by changes in the glass transition temperature, relating to the mobility of macromolecular chains in the amorphous phase and the degree of crystallinity of the films.[12] The crystals behave as charges and physical agents of intercrossing, which tend to reinforce and rigidize the TPS films.[43]

Deformation of TPS-CS and TPS-RS presented an average value of 0.5 mm/mm and 0.1 mm/mm, respectively, when they were exposed to 0% RH. No significant difference in the deformation value was observed when materials were exposed to 33% RH in comparison with the values observed at 0% RH; however, when the TPS were exposed to 55% RH [Figure 7(c)], there was an increase in deformation and this tendency was more evident for the TPS-CS. This increased deformation of the TPS could be attributed to the plasticizing effect of the water molecules and glycerol, which penetrate the polymeric chains, increasing the free volume, improving macromolecular mobility and thus, increasing the deformation. Moreover, this movement brings about a decrease in the interactions between the starch molecules causing them to weaken, thereby reducing tensile strength and the modulus.[29]

It has been reported that the addition of large quantities of plasticizer (30%), which interacts with moisture in the system, tends to reduce both the elastic modulus and resistance to traction while increasing elongation of the TPS, thereby conferring poor mechanical properties, as can be seen in Figure 7, because of the fact that the films are softer and more flexible; this behavior can be explained by the increase in free volume of the starch matrix with which the material tends to approach its glassy transition. Therefore, after a time, the modulus will decrease.[44]

It is relevant to point out that the mechanical properties of TPS experience changes when exposed to external factors such as time, temperature and relative humidity. This is due to internal water plasticizing phenomena and structural retro-degradation resetting experienced by TPS and, according to the literature, this is the main reason for the significant differences between reported values for this type of characterization.[45]

CONCLUSIONS

In the present study, ramon starch was used as the raw material for the manufacture of TPS films as an alternative to TPS-CS.

A dark-colored film of TPS-RS was obtained, which most likely can be attributed to the thermo compression process carried out at a high temperature of 160 °C, which allowed the carbohydrates, proteins and phenolic compounds of the native starch to

intervene in Maillard reactions; however, further research is recommended in order to determine the origin of these colored compounds.

X-ray diffraction analysis showed similar values in residual crystallinity (percentage of crystallinity that remains after plasticization process) in both TPS.

These results were confirmed by FTIR where greater intensity was observed in band at 1016 cm^{-1} in TPS-CS and TPS-RS, in comparison with their corresponding native starches, indicating a higher level of amorphicity in the material. However, in the SEM micrographs it was possible to observe certain remnant granular structures in the TPS-RS. The DMA analysis also showed similar values of T_g (24 °C), in both TPS.

The presence of a large quantity of hydroxyl groups in the FTIR spectrum of TPS-RS gives rise to a poor resistance to water which is confirmed in this study with an increase in water absorption of the TPS to 33 and 55% RH. One way of improving this excessive absorption of water in the material would be to modify the starch from ramon seeds in order to reduce its hydrophilic nature, or to mix TPS-RS with synthetic biodegradable polymers.

At 55% of relative humidity (RH), TPS-RS had higher tensile strength and deformation than TPS-CS. The TPS-RS also presented a slightly higher modulus of elasticity value and a slightly lower deformation value, compared to the TPS-CS, which would suggest that the TPS-RS presents greater resistance to deformation at 55% RH.

These results represent a starting point to potentialize the use of TPS-RS instead of TPS-CS for the development of new biodegradable materials for practical applications in different areas; however, further research must be carried out on the rheological properties, thermal properties by differential scanning calorimetry (DSC) and oxygen barrier properties.

ACKNOWLEDGMENTS

The authors would like to express their gratitude to the Tecnológico Nacional de México, for the financial support for the project 071.14-PD. XRD measurements were performed at LANNBIO Cinvestav Mérida, under support from projects FOMIX-Yucatán 2008-108160 and CONACYT LAB-2009-01 No. 123913. Technical help is acknowledged to MSc Daniel Aguilar. The authors thank Dr. Wilberth Herrera Kao for his technical assistance on FTIR and DMA experiments.

REFERENCES

1. Dang, K. M.; Yoksan, R. *Carbohydr. Polym.* **2015**, *115*, 575.
2. Šimkovic, I. *Carbohydr. Polym.* **2013**, *95*, 697.
3. Prachayawarakorn, J.; Sangnitidej, P.; Boonpasith, P. *Carbohydr. Polym.* **2010**, *81*, 425.
4. Mohammadi Nafchi, A.; Moradpour, M.; Saeidi, M.; Alias, A. K. *Starch–Stärke* **2013**, *65*, 61.
5. Gina, P.; Flores, N. C. *Bioplásticos* **2014**, *27*. 1.
6. Deepika, V.; Jayaram Kumar, K.; Anima, P. *Carbohydr. Polym.* **2013**, *96*, 253.
7. Leyva-Lopez, N. E.; Vasco, N.; Barba de la Rosa, A. P.; Paredes-Lopez, O. *Plant Foods Hum. Nutr.* **1995**, *47*, 49.
8. Pérez, E. E.; Lares, M.; González, Z. M. *Starch–Stärke* **1997**, *49*, 103.
9. Rondán-Sanabria, G. G.; Finardi-Filho, F. *Food Chem.* **2009**, *114*, 492.
10. Pérez-Pacheco, E.; Moo-Huchin, V. M.; Estrada-León, R. J.; Ortiz-Fernández, A.; May-Hernández, L. H.; Ríos-Soberanis, C. R.; Betancur-Ancona, D. *Carbohydr. Polym.* **2014**, *101*, 920.
11. Moo-Huchin, V. M.; Cabrera-Sierra, M. J.; Estrada-León, R. J.; Ríos-Soberanis, C. R.; Betancur-Ancona, D.; Chel-Guerrero, L.; Ortiz-Fernández, A.; Estrada-Mota, I. A.; Pérez-Pacheco, E. *Food Hydrocolloids* **2015**, *45*, 48.
12. Halley, P.; Rutgers, R.; Coombs, S.; Kettels, J.; Gralton, J.; Christie, G.; Jenkins, M.; Beh, H.; Griffin, K.; Jayasekara, R.; Lonergan, G. *Starch–Stärke* **2001**, *53*, 362.
13. Ma, X.; Chang, P. R.; Yu, J.; Stumborg, M. *Carbohydr. Polym.* **2009**, *75*, 1.
14. Averous, L.; Boquillon, N. *Carbohydr. Polym.* **2004**, *56*, 111.
15. Teixeira, E. M.; Da Róz, A. L.; Carvalho, A. J. F.; Curvelo, A. A. S. *Carbohydr. Polym.* **2007**, *69*, 619.
16. Róz, A. L. D.; Carvalho, A. J. F.; Gandini, A.; Curvelo, A. A. S. *Carbohydr. Polym.* **2006**, *63*, 417.
17. Yan, Q.; Hou, H.; Guo, P.; Dong, H. *Carbohydr. Polym.* **2012**, *87*, 707.
18. Zhang, K.; Ran, X.; Zhuang, Y.; Yao, B.; Dong, L. *Chem. Res. Chin. U* **2009**, *25*, 748.
19. Huang, M.; Yu, J.; Ma, X. *Polym. Degrad. Stab.* **2005**, *90*, 501.
20. Ma, X. F.; Yu, J. G.; Wan, J. J. *Carbohydr. Polym.* **2006**, *64*, 267.
21. Nara, S.; Komiya, T. *Starch–Stärke* **1983**, *35*, 407.
22. Zhang, Y.; Rempel, C.; Liu, Q. *Crit. Rev. Food Sci. Nutr.* **2014**, *54*, 1353.
23. Mali, S.; Sakanaka, L. S.; Yamashita, F.; Grossmann, M. V. E. *Carbohydr. Polym.* **2005**, *60*, 283.
24. Curvelo, A. A. S.; de Carvalho, A. J. F.; Agnelli, J. A. M. *Carbohydr. Polym.* **2001**, *45*, 183.
25. Chen, C. H.; Kuo, W. S.; Lai, L. S. *Food Hydrocolloids* **2009**, *23*, 714.
26. Yakimets, I.; Paes, S. S.; Wellner, N.; Smith, A. C.; Wilson, R. H.; Mitchell, J. R. *Biomacromolecules* **2007**, *8*, 1710.
27. Iriani, E. S.; Sunarti, T. C.; Richana, N.; Mangunwidjaja, D.; Hadiyoso, A. *Procedia Chem.* **2012**, *4*, 245.
28. Tako, M.; Hizukuri, S. *Carbohydr. Polym.* **2002**, *48*, 397.
29. van Soest, J. J. G.; Benes, K.; de Wit, D.; Vliegenthart, J. F. G. *Polymer* **1996**, *37*, 3543.
30. Silverstein, R. M.; Bassler, G. C. *J. Chem. Edu.* **1962**, *39*, 546.
31. Lomelí-Ramírez, M. G.; Barrios-Guzmán, A. J.; García-Enriquez, S.; de Jesús Rivera-Prado, J.; Manríquez-González, R. *BioResources* **2014**, *9*, 2960.

32. Mahieu, A.; Terrié, C.; Agoulon, A.; Leblanc, N.; Youssef, B. *J. Polym. Res.* **2013**, *20*, 1.

33. Mahieu, A.; Terrié, C.; Youssef, B. *Ind. Crops Prod.* **2015**, *72*, 192.

34. Cyras, V. P.; Manfredi, L. B.; Ton-That, M. T.; Vázquez, A. *Carbohydr. Polym.* **2008**, *73*, 55.

35. Jiang, W.; Qiao, X.; Sun, K. *Carbohydr. Polym.* **2006**, *65*, 139.

36. Karagoz, S.; Ozkoc, G. *Polym. Eng. Sci.* **2013**, *53*, 2183.

37. Cyras, V. P.; Tolosa Zenklusen, M. C.; Vazquez, A. *J. Appl. Polym. Sci.* **2006**, *101*, 4313.

38. Wilhelm, H. M.; Sierakowski, M. R.; Souza, G. P.; Wypych, F. *Carbohydr. Polym.* **2003**, *52*, 101.

39. Lourdin, D.; Bizot, H.; Colonna, P. *J. Appl. Polym. Sci.* **1997**, *63*, 1047.

40. Rodriguez-Gonzalez, F. J.; Ramsay, B. A.; Favis, B. D. *Carbohydr. Polym.* **2004**, *58*, 139.

41. Sarazin, P.; Li, G.; Orts, W. J.; Favis, B. D. *Polymer* **2008**, *49*, 599.

42. Chaleat, C.; Halley, P.; Truss, R. *Starch Polym.* **2014**, 2103.

43. Bertolini, A. Starches: Characterization, Properties, and Applications; Boca Raton, FL: CRC Press, **2009**.

44. Benczédi, D. *Trends Food Sci. Technol.* **1999**, *10*, 21.

45. Mina, H. J. H., Biotecnología en el Sector Agropecuario y Agroindustrial **2012**, 10, 99.